

Negative charge-transfer energy in SrFeO₃ revisited with hard x-ray photoemission spectroscopy

D. Takegami ^{1,2} M. Nakamura,¹ A. Melendez-Sans ² K. Fujinuma ¹ R. Nakamura,¹ M. Yoshimura,³ K.-D. Tsuei,³ A. Tanaka ⁴ M. Gen ⁵ Y. Tokunaga,⁶ S. Ishiwata ⁷ and T. Mizokawa ¹

¹Department of Applied Physics, Waseda University, Shinjuku, Tokyo 169-8555, Japan

²Max Planck Institute for Chemical Physics of Solids, 01187 Dresden, Germany

³National Synchrotron Radiation Research Center, 30076 Hsinchu, Taiwan

⁴Department of Quantum Matter, ADSM, Hiroshima University, Higashi-Hiroshima 739-8530, Japan

⁵RIKEN Center for Emergent Matter Science (CEMS), Wako, Saitama 351-0198, Japan

⁶Department of Advanced Materials, University of Tokyo, Kashiwa Chiba 277-8561, Japan

⁷Division of Materials Physics, Graduate School of Engineering Science, Osaka University, Osaka 560-8531, Japan



(Received 15 April 2024; accepted 7 June 2024; published 20 June 2024)

We report hard x-ray photoelectron spectroscopy on SrFeO₃ which is one of the classical conducting transition-metal oxides with a noncollinear magnetic structure. The obtained spectra show a detailed charge-transfer (CT) satellite structure, the Fe 2p_{3/2} main peak exhibits multiplet splitting, and the deterioration signs present in previous reports are absent here, allowing for a better determination of its intrinsic electronic structure. The results are well described by a FeO₆ cluster model with a charge-transfer energy of about −1.0 eV, confirming the values obtained in the previous works. The negative CT energy indicates that the electronic configuration of the tetravalent Fe is d⁵L rather than d⁴ where L represents an O 2p hole. The small spectral weight observed at the Fermi level indicates the correlated metallic state with localized Fe 3d electrons and mobile O 2p holes which are governed by a large d-d Coulomb interaction and negative CT energy.

DOI: [10.1103/PhysRevB.109.235138](https://doi.org/10.1103/PhysRevB.109.235138)

I. INTRODUCTION

In high valence transition-metal oxides, oxygen-to-metal charge-transfer (CT) energy frequently becomes negative and the ground state electronic configuration is dominated by dⁿ⁺¹L (L: oxygen 2p hole) rather than dⁿ [1–3]. Since the CT gap is expected to collapse with a negative CT value, such transition-metal oxides tend to be metallic. However, the strong hybridization between the O 2p and transition-metal d orbitals can open an energy gap at the Fermi level in specific lattice geometries [4,5] or under lattice distortions due to charge/orbital ordering [6–8]. In addition, the oxygen 2p holes play important roles in Li_xMO₂ (M = Mn, Co, and Ni) cathodes of Li-ion batteries [9–11].

Among high valence transition-metal oxides, perovskite-type Fe⁴⁺ oxides (with a crystal structure as illustrated in Fig. 1(a)) exhibit rich physical properties including the helical magnetic structure of SrFeO₃ [12–14] and Fe³⁺/Fe⁵⁺ charge disproportionation in CaFeO₃ [15,16]. SrFeO₃ is a good conductor. A high density of states of Fe 3d at the Fermi level is predicted by density functional theory (DFT) calculations with a local density approximation (LDA) [17]. On the other hand, soft x-ray photoemission studies revealed a small spectral weight at the Fermi level [2,18] which is partly

consistent with LDA+U calculations [19]. The cluster-model analysis of the Fe 2p core-level spectra shows negative CT energy [2] which makes the ground state dominated by d⁵L [Fig. 1(b)]. The small spectral weight at the Fermi level originates from the large on-site Coulomb interaction U between Fe 3d electrons. The helical magnetic structure is theoretically explained in a d-p lattice model with negative CT energy [20]. The single-crystal growth of SrFeO₃ [21] provided a new platform to study the transport properties of SrFeO₃, SrFeO_{3-δ}, and SrFe_{1-x}Co_xO₃ under a magnetic field [22–26]. Bilayer Sr₃Fe₂O₇ exhibits an interesting interplay between the helical magnetism and the charge disproportionation Fe³⁺/Fe⁵⁺ [27]. Since the CT energy is negative in the Fe⁴⁺ oxides, the valence change from Fe⁴⁺ to Fe³⁺/Fe⁵⁺ corresponds to d⁵L + d⁵L → d⁵L² + d⁵ rather than d⁴ + d⁴ → d³ + d⁵ [5]. Very recently, the electronic properties of SrFeO₃ with negative CT energy have gained renewed interest due to the emergence of topological spin textures [28]. In addition, the spatial distributions of the Fe 3d electrons have been mapped by the core differential Fourier synthesis of high-resolution x-ray diffraction data, confirming the d⁵L electronic configuration [29].

In this context, it is highly important to study the precise electronic structure of single-crystalline SrFeO₃ by means of bulk-sensitive hard x-ray spectroscopy. The target of this paper is twofold. In correlated electron systems, pictures established by more surface-sensitive soft x-ray photoemission spectroscopy have been challenged by bulk-sensitive hard x-ray photoemission spectroscopy (HAXPES) [31–35]. In the particular case of SrFeO₃, spectral features thought to be from the surface or grain boundary contributions were reported in a previous study by Bocquet *et al.* [2], which still remains as one

Published by the American Physical Society under the terms of the [Creative Commons Attribution 4.0 International](https://creativecommons.org/licenses/by/4.0/) license. Further distribution of this work must maintain attribution to the author(s) and the published article's title, journal citation, and DOI. Open access publication funded by Max Planck Society.

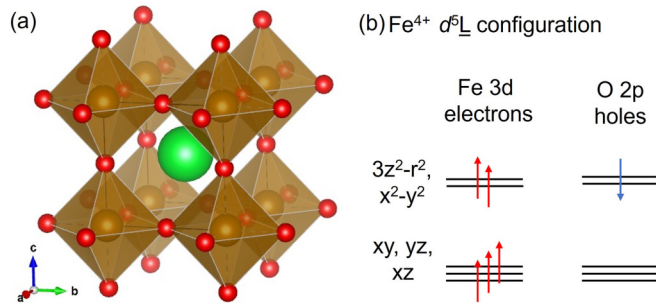


FIG. 1. (a) Crystal structure of SrFeO₃ illustrated by VESTA [30]. The green (red) spheres represent the Sr (O) ions and the brown octahedra correspond to the FeO₆ octahedra. (b) Electronic configuration for the d^5L state of Fe⁴⁺.

of the main works of reference for such systems after more than 30 years since its publication. Thus, there is indeed a need for a bulk-sensitive HAXPES experiment on single-crystalline samples to verify the intrinsic character of the conclusions drawn in the past. The main purpose of this paper is thus to revisit the oxygen hole picture of SrFeO₃ by means of a state-of-the-art HAXPES measurement. The secondary purpose is to provide information of the bulk electronic structure of SrFeO₃ which is currently attracting great interest as an environmentally friendly energy material [36–38]. The present paper reports HAXPES results on high-quality single crystals of SrFeO₃. Detailed line shapes of the Fe 2*p* main peaks and CT satellites are successfully obtained and allow a precise cluster model analysis confirming the negative CT energy. The spectral weight at the Fermi level is clearly observed, suggesting that the O 2*p* states are strongly hybridized with Fe 3*d* near the Fermi level probably preventing the charge disproportionation.

II. METHODS

Single crystals of SrFeO₃ were grown as reported in the literature [21,29]. HAXPES measurements were performed at the Max-Planck-NSRRC HAXPES endstation with a MB Scientific A-1 HE analyzer, Taiwan undulator beamline BL12XU of SPring-8 [39,40]. The photon energy was set to 6.5 keV and the total energy resolution was about 300 meV. The binding energy of the HAXPES spectra was calibrated using the Fermi edge of Au. The x-ray incidence angle was about 15°, and the photoelectron detection angle was 90°. The radius of the beam spot was about 50 μm. The first SrFeO₃ sample was clamped on an aluminum sample holder. A second SrFeO₃ sample was glued to an aluminum sample holder using a commercial Ag epoxy, and was heated at about 100 °C for about 10 min in the air for curing the epoxy. Both samples were coated with a thick layer of carbon paint and were cleaved with a knife cleaver under an ultrahigh vacuum of 10^{−9} mbar at room temperature in order to expose a fresh surface for the measurement and to ensure that no signal would come from the uncleaved regions of the sample. The measurements were performed at 80 K to prevent the degradation of the sample during its exposure to the x rays.

To compute the total and partial (i.e., orbitally resolved) single-particle density of states (DOS, PDOS), we

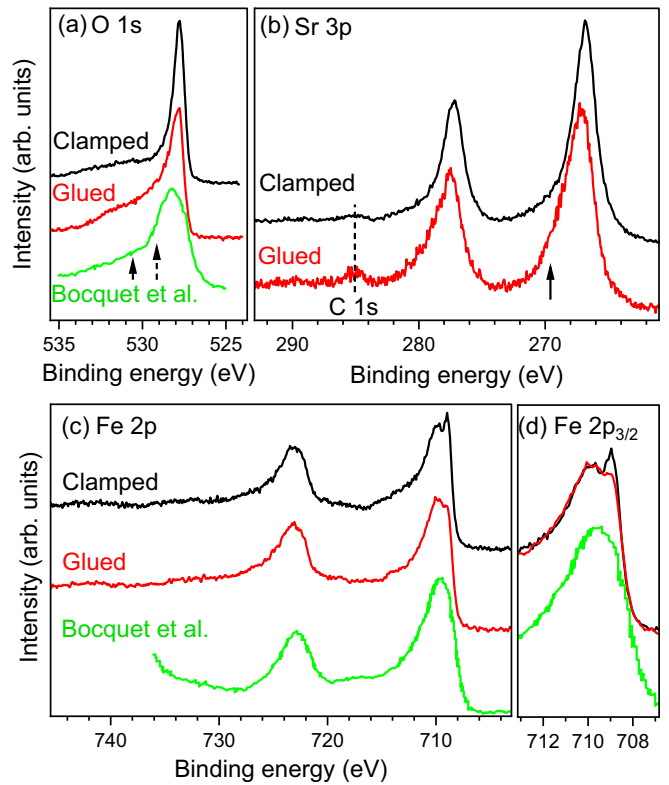


FIG. 2. (a) O 1*s*, (b) Sr 3*p*, and (c) Fe 2*p* core-level spectra of SrFeO₃ from the HAXPES experiments on the clamped (black) and glued (red) samples, together with the spectra from Bonquet *et al.* [2]. (d) Closeup of the Fe 2*p*_{3/2} peak.

performed non-spin-polarized (scalar relativistic) DFT calculations within the LDA using the full-potential local-orbital (FPLO) code [41]. For the Brillouin zone (BZ) integration we used the tetrahedron method with a $12 \times 12 \times 12$ **k** mesh. For the DFT+*U* calculations, the values $U = 2, 4,$ and 6 eV and $J = 1.0$ eV were used. Full multiplet configuration interaction calculations on the FeO₆ cluster model have been performed using the XTLS 9.25 code [42,43]. The initial (final) states are given by linear combinations of d^4 , d^5L , and d^6L^2 (cd^4 , cd^5L , and d^6L^2) configurations in which L represents a hole in the O 2*p* orbitals (and c represents a core hole) [44].

III. CORE LEVELS

Figure 2(a) displays the core-level spectra of O 1*s*. We observe that the clamped sample displays a sharp and intense main peak, followed by a weak feature on the higher binding energy side at around 532 eV, likely originating from the carbon paint, slightly visible also in Fig. 2(b) next to the Sr 3*p*. The glued sample, however, displays a broader, highly asymmetric main peak with a large tail, similar to the soft XPS spectra on polycrystalline samples reported in Bocquet *et al.* [2] or from *ex situ* measurements on thin films [45]. This indicates that the oxygen ions in the glued sample are not all in a single, equivalent chemical environment, suggesting already the possibility of some form of degradation or oxygen loss as we will discuss later.

Figure 2(b) displays the Sr 3*p* spectra. The clamped sample displays a sharper and more symmetric peak line shape, while in the glued sample, the peak is broader and more asymmetric, indicating the presence of a different Sr component as well. This is also similar with the observation in the Sr 3*d* core-level spectra in Bocquet *et al.*, where an additional Sr component is required to explain the experimental spectra.

As shown in Fig. 2(c), the Fe 2*p* spectrum of the clamped sample exhibits richer and more detailed spectral features than the glued one or in the previous works in the literature [2,45]. The main line of Fe 2*p*_{3/2} [Fig. 2(d)] exhibits a double-peak structure which is not observed either in the previous work or in the glued sample. Here, we note in particular that in the clamped and glued samples the main peaks show otherwise a matching width, indicating that the disappearance of the lower-energy peak is not due to a simple spectral broadening. Furthermore, a more detailed and clear charge-transfer satellite structure is observed. We can then make use of the more detailed spectral features from the spectrum of the clamped sample and analyze them with a FeO₆ configuration interaction full multiplet cluster model as described below.

Starting with the CT energy Δ , shown in Fig. 3(a), changes in Δ result in changes mainly in the double-peak structure of the main peak line shape. Overall, the satellite position and shapes are not too sensitive to the differences between a small, but positive, Δ (where the ground state is already dominated by a d^5L configuration) to more negative values. However, the observation of the double-peak structure allows a finer tuning, as larger values of Δ result in splittings that are beyond that in the experimental spectra. The position of the double-peak structure is best reproduced with a value of around $\Delta = -1$ eV. Some details, such as the asymmetries of some features, are not captured in the cluster model, and can be attributed to the simplified description of the ligand states, with a bandlike description [35] or the use of dynamical mean-field theory (DMFT) being necessary to reproduce them. Next, we show in Fig. 3(b) a parameter sweep for the Fe-O transfer integral V_{eg} . Here, we observe that the position of the satellite features are extremely sensitive to V_{eg} . In our HAXPES spectra, as discussed earlier, we can observe in more detail the satellite structures, such as the small bump followed by a dip in A, or the higher energy satellites B₁ and B₂. Those structures, present in our simple cluster model calculations, can be once again used to finely determine the parameter values, with a value of around $V_{eg} = -2.4$ eV providing the best match. From the optimized parameter values [43] we obtain a ground state that has 24.5% d^4 , 63.2% d^5L , and 12.3% d^6L^2 , consistent with the dominant d^5L character regularly reported in the literature [2,29,46,47], and with an average Fe occupation of 4.88, very close albeit slightly higher than the previously reported range of 4.64–4.8 [29,46,47].

IV. VALENCE BAND

Figure 4(a) shows the valence-band spectrum of SrFeO₃. The spectrum consists of two main broad features, the deeper one from around 7 to 4 eV, and the other one at around 2–3 eV. On the lower-energy side, a tail extends from around 2 eV up to the Fermi energy. Similar to the measurements from the literature at lower photon energies [2,45] our bulk-sensitive

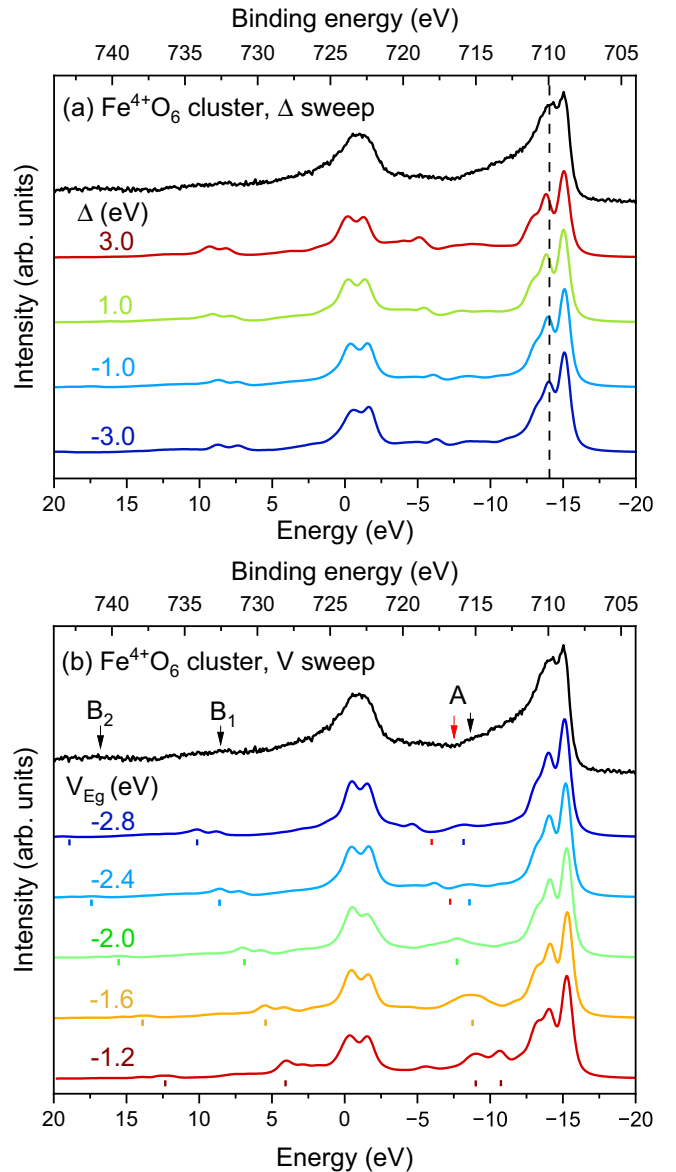


FIG. 3. Experimental Fe 2*p* HAXPES spectrum from the clamped sample (black), together with spectra calculated using the FeO₆ cluster model. (a) V_{eg} is fixed to -2.4 and the value of Δ is changed. (b) Δ is fixed to -1.0 and the value of V_{eg} is changed.

HAXPES finds a suppressed but nonzero spectral weight near the Fermi energy, confirming the bulk nature of the almost-gapped electronic structure.

In order to understand the valence-band spectrum, we have performed a variety of calculations. First, Fig. 4(b) shows LDA calculations, where the Fe 3*d* states are predicted to be largely around the Fermi energy. Considering the photoionization cross sections [48] at the 6.5 keV used in our experiment, we see that the O 2*p* contributions are expected to be fully suppressed [Fig. 4(c)], and instead, the small Sr 4*p* contributions form its hybridization with the O 2*p* and the Fe 4*s* are strongly enhanced [40]. However, even after considering the cross sections, we observe that the Fe 3*d* states from the LDA calculations are clearly incompatible with the almost zero weight around the Fermi energy. We can

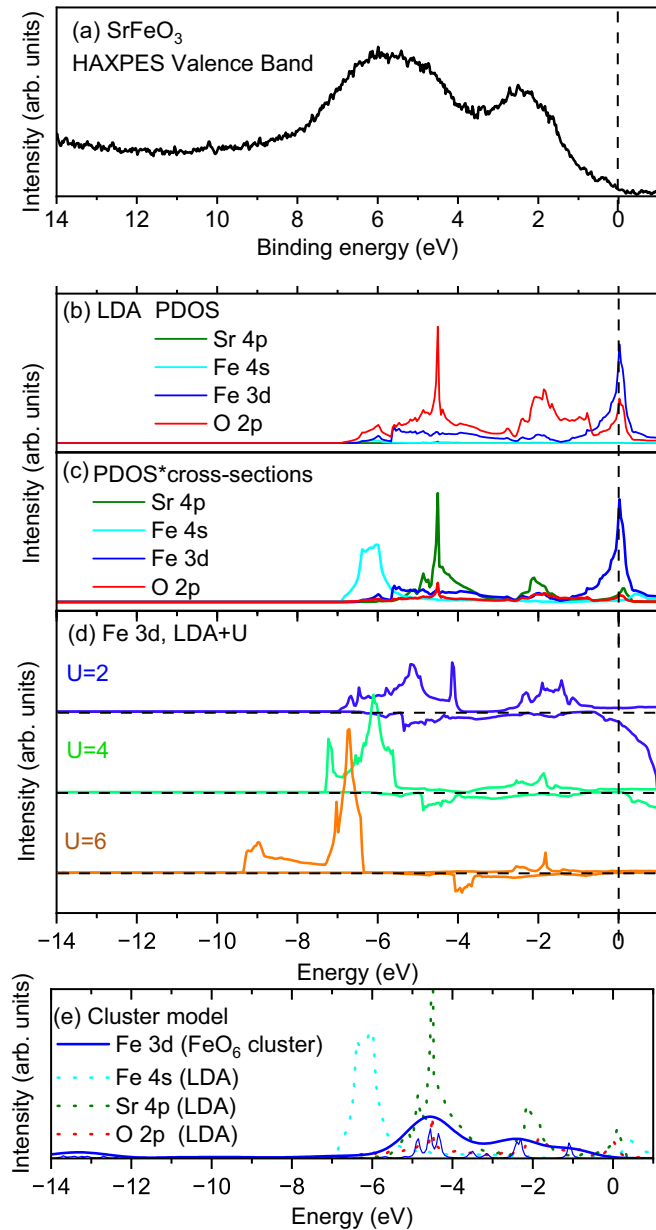


FIG. 4. (a) Valence-band HAXPES spectrum of SrFeO_3 . (b) PDOS of the main relevant contributions calculated by LDA. (c) PDOS multiplied by their respective photoionization cross sections at 6.5 keV. (d) Fe 3d PDOS calculated using LDA+ U ($U = 2, 4, \text{ and } 6$ eV). The contributions displayed with positive intensity correspond to the majority spin and those with negative intensity to the minority spin. (e) Cluster model calculations of the valence band (thick solid line). In the cluster calculations, the Fermi energy has been chosen to match the end of the tail from the first emission feature. The dotted lines show the Fe 4s, Sr 4p, and O 2p PDOS from LDA after the inclusion of cross sections, and the Fe 3d are scaled to match the integrated intensity of the Fe 3d occupied PDOS after the inclusion of cross sections to allow for a better comparison with the LDA.

simulate the effects of correlations by performing LDA+ U , as shown in Fig. 4(d). We observe that even small values of U are able to shift the Fe 3d states away from the Fermi energy, indicating thus the importance of correlation effects

to understand the valence structure. However, as is often seen in LDA+ U calculations for systems with strong correlations, with realistic values of the Coulomb repulsion of around $U = 6$ eV, the states are pushed too deep to be compatible with the experimental observations. The cluster calculations of the valence band [Fig. 4(e)] performed with the parameters obtained from the core-level study, however, provide a Fe 3d spectrum that is more compatible with the experimental structure, by providing, together with the Sr 4p, a spectral weight between -5 eV and the Fermi energy and the uncorrelated Fe 4s states accounting for the remaining spectral weight at around -6 eV. The good solution provided by the cluster model indicates that even for the valence Fe 3d electrons, the local environment and interactions might dominate over longer-ranged band formations.

V. DISCUSSIONS

A comparison of the spectra observed from the glued (i.e., lightly heat treated) and the clamped sample shows several differences that are compatible with some form of sample degradation, such as oxygen loss. As the heating was performed *ex situ* before the *in situ* cleave previous to the measurement, this indicates that the relatively short, mild heating does not only affect near the surfaces but also the bulk of the material. The use of epoxy glues that require thermal treatment for curing is a very commonly used sample preparation for a wide variety of experimental techniques, and from our results, we find that alternative methods might be best to study the intrinsic electronic structure or properties of SrFeO_3 .

In the Fe 2p core-level spectrum of the clamped sample, we observe a double-peak structure in the $2p_{3/2}$ main line as well as clear satellite features. Such double-peak structures have also been observed in octahedrally coordinated Fe^{2+} and Fe^{3+} [49,50] and successfully explained with the multiplet structures [51,52]. However, they often fail to materialize in other experimental studies, resulting in displaying only a single peak, with surface effects, oxygen deficiencies, mixing of other Fe valencies, etc., being suggested as some of the possible causes [49,50]. The clear observation of the double peak is thus an indication of a pure system. This is consistent with our results on SrFeO_3 , where the glued, degraded sample does not display the splitting. Similarly, the spectra reported in Bocquet *et al.*'s work [2] did not present the double-peak structure, and did feature similar trends observed on the glued sample compatible with some form of degradation, suggesting that heat treatments or the less-bulk-sensitive character of the measurements might have affected the spectra.

Nevertheless, the conclusions obtained from the cluster model calculations using the additional details observed in our spectra do not significantly deviate from those of the past studies, indicating that, while there are degradation/surface differences detectable with spectroscopy, those might either be very minor or their effects on the Fe electronic states not too significant.

Finally, the HAXPES valence-band spectrum confirms that the suppression at the Fermi energy is intrinsic from the bulk. This, once again, highlights the importance of correlation effects, with the agreement of the cluster results indicating

that indeed the Fe 3*d* states are relatively localized. Thus, it is to be expected that the oxygen holes left by the negative CT energy play an important role in the metallicity of the system.

VI. CONCLUSIONS

In conclusion, we have revisited the electronic structure of SrFeO₃ by means of HAXPES. The spectra on samples that were not heated during their preparation display cleaner spectra without the signatures that can be attributed to some form of degradation. More detailed features are found, including the multiplet splitting on the Fe 2*p*_{3/2} main peak. By using a Fe⁴⁺O₆ cluster model, we confirm a negative CT energy of about -1.0 eV, with *d*⁵*L* as the dominant configuration. The results do not significantly deviate much from past results from samples that show signs of degradation, indicating that those effects might be very minor or not significantly affect the Fe electronic states. Finally, the small spectral weight at the Fermi level observed in the valence band indicates a correlated metallic state with the localized Fe 3*d* electrons and the mobile O 2*p* holes which are governed by the large *d-d* Coulomb interaction and the negative CT energy.

ACKNOWLEDGMENTS

D.T. acknowledges the support by the Deutsche Forschungsgemeinschaft (DFG, German Research Foundation) under the Walter Benjamin Programme, Projektnummer

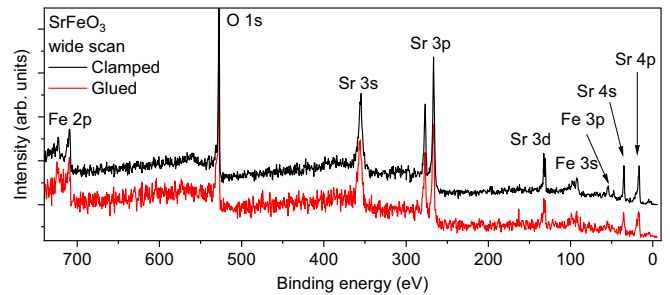


FIG. 5. HAXPES wide scans taken at 6.5 keV of the glued and clamped samples.

521584902. The HAXPES measurements were facilitated by the Max Planck-POSTECH-Hsinchu Center for Complex Phase Materials. This work was supported by Grants-in-Aid from the Japan Society of the Promotion of Science (JSPS) (No. JP22H01172, No. JP23K13068, and No. JP22H00343).

APPENDIX

The wide scans of the two samples of SrFeO₃ are displayed in Fig. 5. The core-level peaks of O 1*s*, Sr 3*s*/3*p*/3*d*/4*s*/4*p*, and Fe 2*p*/3*s*/3*p* are observed, as expected from the composition, with no other element impurities (other than some carbon, as discussed in the main text) detected.

- [1] T. Mizokawa, H. Namatame, A. Fujimori, K. Akeyama, H. Kondoh, H. Kuroda, and N. Kosugi, Origin of the band gap in the negative charge-transfer-energy compound NaCuO₂, *Phys. Rev. Lett.* **67**, 1638 (1991).
- [2] A. E. Bocquet, A. Fujimori, T. Mizokawa, T. Saitoh, H. Namatame, S. Suga, N. Kimizuka, Y. Takeda, and M. Takano, Electronic structure of SrFe⁴⁺O₃ and related Fe perovskite oxides, *Phys. Rev. B* **45**, 1561 (1992).
- [3] M. A. Korotin, V. I. Anisimov, D. I. Khomskii, and G. A. Sawatzky, CrO₂: A self-doped double exchange ferromagnet, *Phys. Rev. Lett.* **80**, 4305 (1998).
- [4] S. Nimkar, D. D. Sarma, H. R. Krishnamurthy, and S. Ramasesha, Mean-field results of the multiple-band extended Hubbard model for the square-planar CuO₂ lattice, *Phys. Rev. B* **48**, 7355 (1993).
- [5] T. Mizokawa, A. Fujimori, H. Namatame, K. Akeyama, and N. Kosugi, Electronic structure of the local-singlet insulator NaCuO₂, *Phys. Rev. B* **49**, 7193 (1994).
- [6] T. Mizokawa, D. I. Khomskii, and G. A. Sawatzky, Spin and charge ordering in self-doped Mott insulators, *Phys. Rev. B* **61**, 11263 (2000).
- [7] S. Johnston, A. Mukherjee, I. Elfimov, M. Berciu, and G. A. Sawatzky, Charge disproportionation without charge transfer in the rare-earth-element nickelates as a possible mechanism for the metal-insulator transition, *Phys. Rev. Lett.* **112**, 106404 (2014).
- [8] R. J. Green, M. W. Haverkort, and G. A. Sawatzky, Bond disproportionation and dynamical charge fluctuations in the perovskite rare-earth nickelates, *Phys. Rev. B* **94**, 195127 (2016).
- [9] T. Mizokawa, Y. Wakisaka, T. Sudayama, C. Iwai, K. Miyoshi, J. Takeuchi, H. Wadati, D. G. Hawthorn, T. Z. Regier, and G. A. Sawatzky, Role of oxygen holes in Li_xCoO₂ revealed by soft x-ray spectroscopy, *Phys. Rev. Lett.* **111**, 056404 (2013).
- [10] R. J. Green, H. Wadati, T. Z. Regier, A. J. Achkar, C. McMahon, J. P. Clancy, H. A. Dabkowska, B. D. Gaulin, G. A. Sawatzky, and D. G. Hawthorn, Evidence for bond-disproportionation in LiNiO₂ from x-ray absorption spectroscopy, [arXiv:2011.06441](https://arxiv.org/abs/2011.06441).
- [11] K. Morita, M. Itoda, E. Hosono, D. Asakura, M. Okubo, Y. Takagi, A. Yasui, N. L. Saini, and T. Mizokawa, Effect of oxygen hole in Li₂MnO₃ revealed by hard x-ray photoemission spectroscopy and band structure calculations, *J. Phys. Soc. Jpn.* **92**, 014702 (2023).
- [12] J. B. MacChesney, R. C. Sherwood, and J. F. Potter, Electric and magnetic properties of the strontium ferrates, *J. Chem. Phys.* **43**, 1907 (1965).
- [13] T. Takeda, Y. Yamaguchi, and H. Watanabe, Magnetic structure of SrFeO₃, *J. Phys. Soc. Jpn.* **33**, 967 (1972).
- [14] T. Takeda and H. Watanabe, Magnetic properties of the system SrCo_{1-x}Fe_xO_{3-y}, *J. Phys. Soc. Jpn.* **33**, 973 (1972).
- [15] M. Takano, N. Nakanishi, Y. Takeda, S. Naka, and T. Takada, Charge disproportionation in CaFeO₃ studied with the Mössbauer effect, *Mater. Res. Bull.* **12**, 923 (1977).
- [16] T. Akao, Y. Azuma, M. Usuda, Y. Nishihata, J. Mizuki, N. Hamada, N. Hayashi, T. Terashima, and M. Takano, Charge-ordered state in single-crystalline CaFeO₃ thin film studied by x-ray anomalous diffraction, *Phys. Rev. Lett.* **91**, 156405 (2003).

- [17] S. Mathi Jaya, R. Jagadish, R. S. Rao, and R. Asokamani, Electronic structure and magnetism of SrFeO₃ and SrCoO₃, *Phys. Rev. B* **43**, 13274 (1991).
- [18] J. Matsuno, T. Mizokawa, A. Fujimori, K. Mamiya, Y. Takeda, S. Kawasaki, and M. Takano, Photoemission and Hartree-Fock studies of oxygen-hole ordering in charge-disproportionated La_{1-x}Sr_xFeO₃, *Phys. Rev. B* **60**, 4605 (1999).
- [19] I. R. Shein, K. I. Shein, V. L. Kozhevnikov, and A. L. Ivanovskii, Band structure and the magnetic and elastic properties of SrFeO₃ and LaFeO₃ perovskites, *Phys. Solid State* **47**, 2082 (2005).
- [20] M. Mostovoy, Helicoidal ordering in iron perovskites, *Phys. Rev. Lett.* **94**, 137205 (2005).
- [21] N. Hayashi, T. Terashima, and M. Takano, Oxygen-holes creating different electronic phases in Fe⁴⁺-oxides: Successful growth of single crystalline films of SrFeO₃ and related perovskites at low oxygen pressure, *J. Mater. Chem.* **11**, 2235 (2001).
- [22] A. Lebon, P. Adler, C. Bernhard, A. V. Boris, A. V. Pimenov, A. Maljuk, C. T. Lin, C. Ulrich, and B. Keimer, Magnetism, charge order, and giant magnetoresistance in SrFeO_{3-δ} single crystals, *Phys. Rev. Lett.* **92**, 037202 (2004).
- [23] P. Adler, A. Lebon, V. Damjanović, C. Ulrich, C. Bernhard, A. V. Boris, A. Maljuk, C. T. Lin, and B. Keimer, Magnetoresistance effects in SrFeO_{3-δ}: Dependence on phase composition and relation to magnetic and charge order, *Phys. Rev. B* **73**, 094451 (2006).
- [24] S. Ishiwata, M. Tokunaga, Y. Kaneko, D. Okuyama, Y. Tokunaga, S. Wakimoto, K. Kakurai, T. Arima, Y. Taguchi, and Y. Tokura, Versatile helimagnetic phases under magnetic fields in cubic perovskite SrFeO₃, *Phys. Rev. B* **84**, 054427 (2011).
- [25] Y. W. Long, Y. Kaneko, S. Ishiwata, Y. Tokunaga, T. Matsuda, H. Wadati, Y. Tanaka, S. Shin, Y. Tokura, and Y. Taguchi, Evolution of magnetic phases in single crystals of SrFe_{1-x}Co_xO₃ solid solution, *Phys. Rev. B* **86**, 064436 (2012).
- [26] S. Chakraverty, T. Matsuda, H. Wadati, J. Okamoto, Y. Yamasaki, H. Nakao, Y. Murakami, S. Ishiwata, M. Kawasaki, Y. Taguchi, Y. Tokura, and H. Y. Hwang, Multiple helimagnetic phases and topological Hall effect in epitaxial thin films of pristine and co-doped SrFeO₃, *Phys. Rev. B* **88**, 220405(R) (2013).
- [27] J.-H. Kim, A. Jain, M. Reehuis, G. Khaliullin, D. C. Peets, C. Ulrich, J. T. Park, E. Faulhaber, A. Hoser, H. C. Walker, D. T. Adroja, A. C. Walters, D. S. Inosov, A. Maljuk, and B. Keimer, Competing exchange interactions on the verge of a metal-insulator transition in the two-dimensional spiral magnet Sr₃Fe₂O₇, *Phys. Rev. Lett.* **113**, 147206 (2014).
- [28] S. Ishiwata, T. Nakajima, J.-H. Kim, D. S. Inosov, N. Kanazawa, J. S. White, J. L. Gavilano, R. Georgii, K. M. Seemann, G. Brandl, P. Manuel, D. D. Khalyavin, S. Seki, Y. Tokunaga, M. Kinoshita, Y. W. Long, Y. Kaneko, Y. Taguchi, T. Arima, B. Keimer *et al.*, Emergent topological spin structures in the centrosymmetric cubic perovskite SrFeO₃, *Phys. Rev. B* **101**, 134406 (2020).
- [29] S. Kitou, M. Gen, Y. Nakamura, K. Sugimoto, Y. Tokunaga, S. Ishiwata, and T. Arima, Real-space observation of ligand hole state in cubic perovskite SrFeO₃, *Adv. Sci.* **10**, 2302839 (2023).
- [30] K. Momma and F. Izumi, VESTA3 for three-dimensional visualization of crystal, volumetric and morphology data, *J. Appl. Crystallogr.* **44**, 1272 (2011).
- [31] H. Sato, K. Shimada, M. Arita, K. Hiraoka, K. Kojima, Y. Takeda, K. Yoshikawa, M. Sawada, M. Nakatake, H. Namatame, M. Taniguchi, Y. Takata, E. Ikenaga, S. Shin, K. Kobayashi, K. Tamasaku, Y. Nishino, D. Miwa, M. Yabashi, and T. Ishikawa, Valence transition of YbInCu₄ observed in hard x-ray photoemission spectra, *Phys. Rev. Lett.* **93**, 246404 (2004).
- [32] M. Taguchi, A. Chainani, K. Horiba, Y. Takata, M. Yabashi, K. Tamasaku, Y. Nishino, D. Miwa, T. Ishikawa, T. Takeuchi, K. Yamamoto, M. Matsunami, S. Shin, T. Yokoya, E. Ikenaga, K. Kobayashi, T. Mochiku, K. Hirata, J. Hori, K. Ishii *et al.*, Evidence for suppressed screening on the surface of high temperature La_{2-x}Sr_xCuO₄ and Nd_{2-x}Ce_xCuO₄ superconductors, *Phys. Rev. Lett.* **95**, 177002 (2005).
- [33] M. Taguchi, A. Chainani, S. Ueda, M. Matsunami, Y. Ishida, R. Eguchi, S. Tsuda, Y. Takata, M. Yabashi, K. Tamasaku, Y. Nishino, T. Ishikawa, H. Daimon, S. Todo, H. Tanaka, M. Oura, Y. Senba, H. Ohashi, and S. Shin, Temperature dependence of magnetically active charge excitations in magnetite across the Verwey transition, *Phys. Rev. Lett.* **115**, 256405 (2015).
- [34] D. Takegami, C.-Y. Kuo, K. Kasebayashi, J.-G. Kim, C. F. Chang, C. E. Liu, C. N. Wu, D. Kasinathan, S. G. Altendorf, K. Hofer, F. Meneghin, A. Marino, Y. F. Liao, K. D. Tsuei, C. T. Chen, K.-T. Ko, A. Günther, S. G. Ebbinghaus, J. W. Seo, D. H. Lee *et al.*, CaCu₃Ru₄O₁₂: A high-Kondo-temperature transition-metal oxide, *Phys. Rev. X* **12**, 011017 (2022).
- [35] D. Takegami, A. Tanaka, S. Agrestini, Z. Hu, J. Weinen, M. Rotter, C. Schüßler-Langeheine, T. Willers, T. C. Koethe, T. Lorenz, Y. F. Liao, K. D. Tsuei, H.-J. Lin, C. T. Chen, and L. H. Tjeng, Paramagnetic LaCoO₃: A highly inhomogeneous mixed spin-state system, *Phys. Rev. X* **13**, 011037 (2023).
- [36] M. L. Tummino, E. Laurenti, F. Deganello, A. Bianco Prevot, and G. Magnacca, Revisiting the catalytic activity of a doped SrFeO₃ for water pollutants removal: Effect of light and temperature, *Appl. Catal. B: Environ.* **207**, 174 (2017).
- [37] S. Gabra, E. J. Marek, S. Poulston, G. Williams, and J. S. Dennis, The use of strontium ferrite perovskite as an oxygen carrier in the chemical looping epoxidation of ethylene, *Appl. Catal. B: Environ.* **286**, 119821 (2021).
- [38] F. Sarikhani, A. R. Soleymani, M. Naseri, and A. Zabardasti, Synthesis of *p-n* heterojunction SrFeO_{3-x}/TiO₂ via thermal treatment/hydrolysis precipitation method with enhanced visible-light activity, *J. Mater. Sci.: Mater. Electron.* **33**, 5790 (2022).
- [39] J. Weinen, T. C. Koethe, C. F. Chang, S. Agrestini, D. Kasinathan, Y. F. Liao, H. Fujiwara, C. Schüßler-Langeheine, F. Strigari, T. Haupricht, G. Panaccione, F. Offi, G. Monaco, S. Huotari, K.-D. Tsuei, and L. H. Tjeng, Polarization dependent hard x-ray photoemission experiments for solids: Efficiency and limits for unraveling the orbital character of the valence band, *J. Electron Spectrosc. Relat. Phenom.* **198**, 6 (2015).
- [40] D. Takegami, L. Nicolai, T. C. Koethe, D. Kasinathan, C. Y. Kuo, Y. F. Liao, K. D. Tsuei, G. Panaccione, F. Offi, G. Monaco, N. B. Brookes, J. Minár, and L. H. Tjeng, Valence band hard x-ray photoelectron spectroscopy on *3d* transition-metal oxides containing rare-earth elements, *Phys. Rev. B* **99**, 165101 (2019).
- [41] K. Koepernik and H. Eschrig, Full-potential nonorthogonal local-orbital minimum-basis band-structure scheme, *Phys. Rev. B* **59**, 1743 (1999).

- [42] A. Tanaka and T. Jo, Resonant $3d$, $3p$, and $3s$ photoemission in transition metal oxides predicted at $2p$ threshold, *J. Phys. Soc. Jpn.* **63**, 2788 (1994).
- [43] For the full multiplet configuration interaction calculations on the FeO₆, the following parameters were used (in eV) unless otherwise indicated: $U_{dd} = 6$, $U_{cd} = 7.6$, $\Delta = -1$, $V_{eg} = 2.4$, $V_{12g} = V_{eg}/2$, $10Dq = 0.5$. The initial (final) states are given by linear combinations of d^4 , d^5L , and d^6L^2 (cd^4 , cd^5L , and d^6L^2). The Slater integrals were obtained from Cowan's code [53] and reduced to the 80% from their atomic values.
- [44] F. M. F. de Groot, J. C. Fuggle, B. T. Thole, and G. A. Sawatzky, $2p$ x-ray absorption of $3d$ transition-metal compounds: An atomic multiplet description including the crystal field, *Phys. Rev. B* **42**, 5459 (1990).
- [45] L. Wang, Y. Du, P. V. Sushko, M. E. Bowden, K. A. Stoerzinger, S. M. Heald, M. D. Scafetta, T. C. Kaspar, and S. A. Chambers, Hole-induced electronic and optical transitions in La_{1-x}Sr_xFeO₃ epitaxial thin films, *Phys. Rev. Mater.* **3**, 025401 (2019).
- [46] T. Saitoh, A. E. Bocquet, T. Mizokawa, and A. Fujimori, Systematic variation of the electronic structure of $3d$ transition-metal compounds, *Phys. Rev. B* **52**, 7934 (1995).
- [47] M. Abbate, G. Zampieri, J. Okamoto, A. Fujimori, S. Kawasaki, and M. Takano, X-ray absorption of the negative charge-transfer material SrFe_{1-x}Co_xO₃, *Phys. Rev. B* **65**, 165120 (2002).
- [48] M. B. Trzhaskovskaya and V. G. Yarzhevsky, Dirac-Fock photoionization parameters for HAXPES applications, *At. Data Nucl. Data Tables* **119**, 99 (2018).
- [49] T. Droubay and S. A. Chambers, Surface-sensitive Fe $2p$ photoemission spectra for α -Fe₂O₃(0001): The influence of symmetry and crystal-field strength, *Phys. Rev. B* **64**, 205414 (2001).
- [50] S. G. Altendorf, D. Takegami, A. Meléndez-Sans, C. F. Chang, M. Yoshimura, K. D. Tsuei, A. Tanaka, M. Schmidt, and L. H. Tjeng, Electronic structure of the Fe²⁺ compound FeWO₄: A combined experimental and theoretical x-ray photoelectron spectroscopy study, *Phys. Rev. B* **108**, 085119 (2023).
- [51] P. S. Bagus, C. J. Nelin, C. R. Brundle, N. Lahiri, E. S. Iltou, and K. M. Rosso, Analysis of the Fe $2p$ XPS for hematite α -Fe₂O₃: Consequences of covalent bonding and orbital splittings on multiplet splittings, *J. Chem. Phys.* **152**, 014704 (2020).
- [52] J. J. Kas, J. J. Rehr, and T. P. Devereaux, *Ab initio* multiplet-plus-cumulant approach for correlation effects in x-ray photoelectron spectroscopy, *Phys. Rev. Lett.* **128**, 216401 (2022).
- [53] A. Kramida, A suite of atomic structure codes originally developed by R. D. Cowan adapted for Windows-based personal computers, National Institute of Standards and Technology, <https://doi.org/10.18434/T4/1502500>, accessed 2024-03-28.